2006

Silicon Oxide Nanoparticles Reveal the Origin of Silicate Grains in Circumstellar Environments

Peneé Armaize Clayborne
Virginia Commonwealth University

SILICON OXIDE NANOPARTICLES AND THE ORIGIN OF SILICATE GRAINS IN CIRCUMSTELLAR ENVIRONMENTS

A Thesis submitted in partial fulfillment of the requirements for the degree of Master of Science at Virginia Commonwealth University.

by

PENEÉ ARMAIZE CLAYBORNE
Bachelor of Science, Radford University, 2002

Director: DR. SHIV N. KHANNA
DEPARTMENT OF PHYSICS

Virginia Commonwealth University
Richmond, Virginia
December 2006

Acknowledgement

I would like to thank God for allowing me the opportunity to further my education at Virginia Commonwealth University. I would also like to give a special thanks to the members as well as those non-members from Saint Paul's Baptist Church and the blessing of Fire on Fridays. If it were not for their giving hearts, I would not have been able to continue my education today. Thank you also goes to Dr. Khanna for allowing me to gain insight from his wisdom and the chance to work with the wonderful gentlemen in his theory group. My last and largest thank you goes to Ayana for her loving support and constant reminders to take a break and eat *real* food.

Table of Contents

List of Figures and Tables

Page

Abstract

SILICON OXIDE NANOPARTICLES REVEAL THE ORGIN OF SILICATE GRAINS IN CIRCUMSTELLAR ENVIRONMENTS

By Peneé Armaize Clayborne

A thesis submitted in partial fulfillment of the requirements for the degree of Master of Science at Virginia Commonwealth University.

Virginia Commonwealth University, 2006

Major Director: Shiv N. Khanna,
Department of Physics

The processes leading to the widespread presence of crystalline silicates throughout the galaxy and the origin of silicon nanoparticles thought to be responsible for the observed extended red emission in diffuse galactic background are still far from being understood. One of the most abundant oxygen bearing species in molecular astronomical regions is SiO. It has been conjectured that silicate formation probably proceeds via the agglomeration of these molecular species; however there are no studies to reveal the microscopic mechanism. We have used a synergistic approach combining experiments in molecular beams and first principles theoretical calculation to demonstrate that the passage

from SiO to SiO_2 proceeds via gradual oxygen enrichment of SinOm clusters and that the smallest cascade involves Si_2O_3, Si_3O_4, Si_4O_5, Si_5O_6 as the intermediate products. We also demonstrate that as the SiO molecules cluster together, the chemistry drives the agglomerates towards configurations such that the central core are pure Si_n clusters while the outer shell are SiO_2 molecules. The gap between the highest occupied molecular orbital and the lowest unoccupied molecular orbital range from 0.84 to 3.84 eV and hence can contribute to the observed extended red emission and blue luminescence. The findings are of general interest in Astrophysics but are also critical to a fundamental understanding of the interstellar extinction.

CHAPTER 1 Introduction

1.1 Silicon Monoxide & Silicates

In chemistry a silicate is a compound containing an anion in which one or more central atoms are surrounded by electronegative ligands. Silicon dioxide (SiO_2), commonly referred to as silica, is sometimes considered a silicate. In geology and astronomy, silicates represent types of rock and nanoparticles as a class of silicon and oxide clusters with a range of oxygen to silicon ratios. Their importance is far reaching in various scientific fields. Silicates can be seen in the form of minerals such as quartz (SiO_2) and forsterite (Mg_2SiO_4) [1], dense cloud material such as porous pyroxenes ($Mg_xFe_{1-x}SiO_3$) [2], and in a multitude of other materials. The formation of these oxygen rich bearing species throughout the galaxy are still far from being understood. It has been proposed the silicate formation in the galaxy occurs by the agglomeration of silicon monoxide in various astronomical regions [3-5].

Silicon Monoxide (SiO) is one of the most abundant molecules in the outflows from oxygen rich stellar sources in which silicon is virtually tied up in the gas phase [6]. The silicate ratio of oxygen to silicon is different form the SiO ratio of 1 to 1 and for SiO_2 is 2 to 1. This brings up important questions: How exactly does the process of oxygen enrichment occur? Is the process of oxygen enrichment a single step process or does the oxygen enrichment occur in a multi-step process?

1.2 Extended Red Emissions & Blue Luminescence

Over the years scientist have been collecting data on the emissions observed from the various astronomical environments [7-9]. These emission features typically give astronomers clues to the composition of various astrophysical environments. One of most debated of these emissions is the Extended Red Emission (ERE).

Since its discovery in the Red Rectangle (HD 44179) [10], these emissions have been observed in a variety of astrophysical environments [11]. Extended Red Emissions are a broad featureless emission band ranging from 540 to 800nm (1.5 eV - 2 eV) and the spectra can be seen in Figure 1.1. The origin of ERE is still highly debated. It has been shown that whatever the source of ERE, it must meet at least two main requirements, 1) it must have a high photoluminescence (PL) efficiency and 2) the emitter must be highly abundant in the interstellar medium [12]. Recently it was discovered that the occurrence of the ERE coexists with a blue luminescence and may be seen as an added requirement for the species at the origin of the ERE [13]. There have been several species hypothesized as the origin of the extended red emissions such as polyaromatic hydrocarbons (PAHs), carbon nanoparticles, C_{60}, and silicon nanoparticles [11-14].

A forerunner for the source of ERE are silicon nanoparticles (SNP) primarily due to silicon's efficient photoluminescence (PL) as seen in semiconductors [15]. This was further emphasized by Zhou et al. illustrating ERE may be possible by silicon nanoparticles, even though it is dipole-forbidden [16]. A second reason for SNP to be a viable candidate for the ERE band is the elemental abundance of silicon (Si) seen in

the interstellar medium (ISM) [11-14]. This leads to the question: If SNPs are the ERE agent, how do SNP form in the ISM from silicon monoxide (SiO) clusters? It has been proposed by Witt *et al.* that $(SiO)_n$ clusters would separate silicon into a core and a SiO_2 sheath that would ultimately result into the formation of SNPs [14]. Even though there have been various studies performed on Si_nO_m clusters as well as various silicates, none have produced a definite theoretical, energetically favorable mechanism for the formation of silicon nanoparticles or silica from the abundant silicon monoxide clusters seen in the interstellar medium.

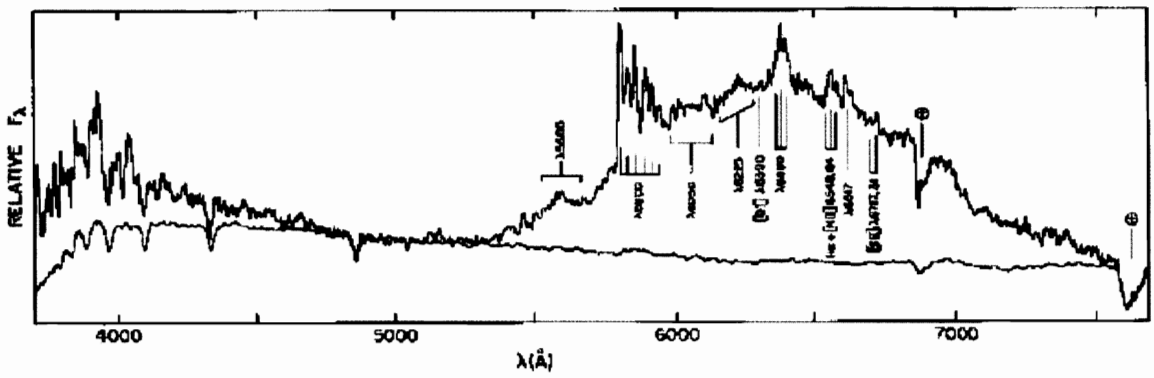

Figure 1.1: Spectra of extended red emissions (ERE). Reference: Schmidt, Cohen, & Margon, 1980, ApJ, 239, L133.

1.3 Technological Applications

Silicon oxide clusters have attracted considerable attention recently from both the experimental and theoretical communities due to their importance in the formation of silicon nanowires (SiNWs) and the optical properties of silicon nanoparticles. It has been shown that gas phase silicon monoxide clusters generated by evaporation sources

play a crucial role in the nucleation and growth of SiNWs [17]. Jia and coworkers fabricated SiNWs by the thermal evaporation of SiO. The nanowires were then studied by energy-dispersive X-ray spectroscopy (EDX) [18]. In order to obtain a higher yield at lower cost, the mechanism for the formation of SiNWs must be better understood. This has led to various theoretical studies of silicon oxide clusters [19-21]. Zhang and coworkers demonstrated theoretically that oxygen atom prefer to exist on the exterior surfaces leaving a silicon core in the interior of various SiO clusters. Their results illustrated that these SiO clusters may facilitate the growth of silicon nanowires [21].

SiO plays an important part in the optical properties of silicon nanocrystrals as well. Recently it was shown that when silicon nanocrystals are embedded in silicon oxide, it has a blue luminescence [22]. Even though this luminescence is much like that of porous silicon (PS), the origin of the strong photoluminescence (PL) is still being debated [23]. If the scientific community can better understand the mechanism of formation, the origin of the blue photoluminescence may be answered.

1.4 Experimental Procedure

Castleman and co-workers generated SiO clusters in beams and studied them in a femtosecond laser based time-of-flight mass spectrometer system equipped with a laser vaporization (LaVa) source (Figure 1.2). The silicon oxide cluster were generated and examined using three different methods. Figure 1.3 illustrates a representative distribution produced from the laser vaporation of SiO solid under an argon environment and photoionized using 1-2 mJ, 800 nm, 50 fs pulses. The product cationic clusters were then analyzed using a typical time-of-flight mass spectrometer. Other experimental methods

were employed including the study of silicon oxide clusters by vaporizing silicon under a helium/oxygen environment and analyzing the resulting clusters, exactly as explained above for comparison purposes.

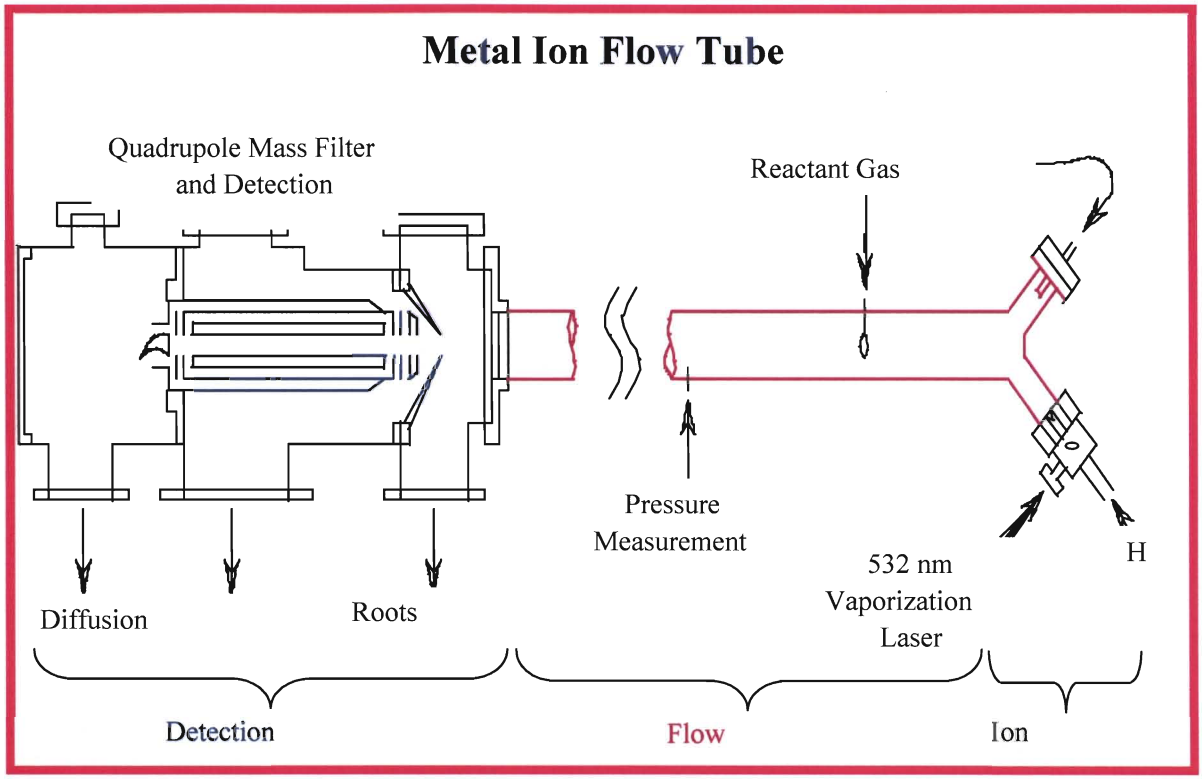

Figure 1.2: Metal Ion flow tube used in experiment to create and detect clusters.

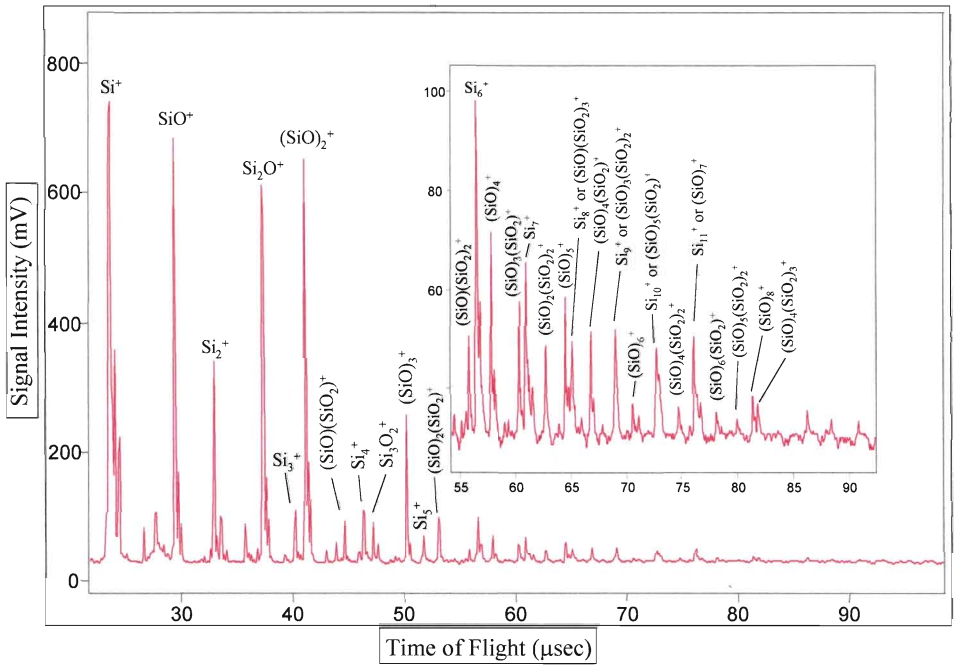

Figure 1.3: Mass spectra of clusters formed by vaporizing solid SiO under argon gas and ionizing the resultant clusters.

CHAPTER 2 Theory

2.1 The Hamiltonian & Statistical Mechanics

The time-independent Schrödinger equation for an isolated N-electron system in the Born-Oppenheimer approximation is given by

$$\hat{H}\Psi = E\Psi \tag{2.1}$$

where E is the electronic energy, Ψ is the wave function and $\hat{H}$ is the Hamiltonian operator. The Hamiltonian for a system of electrons and nuclei is defined as,

$$\hat{\mathrm{H}} = -\frac{\hbar^2}{2m_e}\sum_i \nabla_i^2 - \sum_{i,I}\frac{Z_I e^2}{|r_i - R_I|} + \frac{1}{2}\sum_{i\neq j}\frac{e^2}{|r_i - r_j|} - \sum_I \frac{\hbar^2}{2M_I}\nabla_I^2 + \frac{1}{2}\sum_{I\neq J}\frac{Z_I Z_J e^2}{|R_I - R_J|} \tag{2.2}$$

where electrons are denoted by lower case subscripts and nuclei, with charge Z_I and mass M_I, denoted by upper case subscripts [24]. If we ignore the nuclear kinetic energy, the fundamental Hamiltonian for the theory of electronic structure can be written,

$$\hat{\mathrm{H}} = \hat{\mathrm{T}} + \hat{V}_{ext} + \hat{V}_{\mathrm{int}} + E_{II} \tag{2.3}$$

In order to write the terms in their simplest form, Hartree atomic units $\hbar = m_e = e = 4\pi/\varepsilon_0 = 1$, are adopted. The kinetic energy operator for electrons $\hat{T}$ is defined as,

$$\hat{\mathrm{T}} = \sum_i -\frac{1}{2}\nabla_i^2 \tag{2.4}$$

The potential acting on the electrons due to the nuclei $\hat{V}_{ext}$ and the electron-electron interaction $\hat{V}_{\text{int}}$ are defined as,

$$\hat{V}_{ext} = \sum_{i,I} V_I\left(\left|r_i - R_I\right|\right) \tag{2.5}$$

and

$$\hat{V}_{\text{int}} = \frac{1}{2}\sum_{i \neq j} \frac{1}{\left|r_i - r_j\right|} \tag{2.6}$$

respectively. The final term, E_{II} is the classical interaction of nuclei with one another and any other terms that contribute to the total energy of the system, but are not relevant to the problem of describing the electrons.

The number of electrons per unit volume in an electronic system in a given state is defined as the *electron density*. The electron density $\rho(\mathbf{r})$ can be defined in terms of Ψ as

$$\rho(\mathbf{r}) = N \int \cdots \int \left|\Psi\left(x_1, x_2, \ldots, x_N\right)\right|^2 dx_1, dx_2, \ldots, dx_N \tag{2.7}$$

Then integrating will lead to the total number of electrons for a system,

$$N = \int \rho(r) dr \tag{2.8}$$

From quantum statistical mechanics one can arrive at expression for the energy U, entropy *S*, and the Helmholtz free energy *F*, at any given temperature *T*. The Helmholtz free energy *F* is defined as,

$$F = Tr\hat{\rho}\left(\hat{\mathrm{H}} + \frac{1}{\beta}\ln\hat{\rho}\right) \tag{2.9}$$

where $\beta = 1/k_B T$ and $\hat{\rho}$ is the density matrix. The trace (Tr) is over all states of the system which have a fixed number of particles N. The last term is the entropy term and is the log of the number of possible states of the system. The density matrix contains a general property such that it is positive definite. Thus the correct equilibrium density matrix is the positive definite matrix that minimizes the free energy, namely,

$$\hat{\rho} = \frac{1}{Q} e^{-\beta \hat{\mathrm{H}}} \tag{2.10}$$

where the partition function Z is given by,

$$Q = Tre^{-\beta \hat{\mathrm{H}}} = e^{-\beta F} \tag{2.11}$$

In a grand canonical ensemble [25-26], where the number of particles is allowed to fluctuate around a mean value, the expression is allowed to include the chemical potential μ and the number operator N. The grand partition function Ω is then defined as,

$$\Omega = Tre^{-\beta\left(\hat{\mathrm{H}} - \mu \hat{\mathrm{N}}\right)} \tag{2.12}$$

where the trace is over all states with any particle number, and the new density matrix becomes,

$$\hat{\rho} = \frac{1}{\Omega} e^{-\beta\left(\hat{\mathrm{H}} - \mu \hat{\mathrm{N}}\right)} \tag{2.13}$$

2.2 Hartree Method; Hartree-Fock Approximation

The Hartree method was first applied to atoms in 1927 by Hartree. The one-electron equation,

$$\varepsilon_i \Psi_i(\vec{r}) = -\frac{\hbar^2}{2m}\nabla^2\Psi_i(\vec{r}) - V^{ion}(\vec{r})\Psi_i(\vec{r}) + \left[e^2 \sum_j^{occ} \int d\vec{r}' \left|\Psi_j(\vec{r}')\right|^2 \frac{1}{\left|\vec{r} - \vec{r}'\right|} \right] \Psi_i(\vec{r}) \qquad (2.14)$$

Where V^{ion} is defined as,

$$V^{ion}(\vec{r}) = -Ze^2 \sum_{\vec{R}} \frac{1}{\left|\vec{r} - \vec{R}\right|}. \qquad (2.15)$$

These sets of equations are known as the Hartree equations. These are a set of equations because there is one for each occupied one-electron level. The equations are non-linear and their wave functions and energies are solved by iteration. This is done by guessing a form for the potential energy term in brackets (V^{el}) on which the equations are solved. A new V^{el} is then computed from the resulting wavefunctions and a new Schrödinger equation is solved. This process continues until further iterations do not alter the potential. This is a *self-consistent* field approximation [27].

The Hartree equations do not take into account the antisymmetric property of the electrons. In 1930 Fock introduced an approximation referred to the Hartree-Fock approximation. In this approach the antisymmetric determinant wavefunction is written for a fixed number *N* of electrons and one finds the single determinant that minimizes the total energy for the full interacting Hamiltonian (2.2). The resulting N x N Slater determinant is,

$$\Phi(\vec{r}_1 s_1, \vec{r}_2 s_2, ..., \vec{r}_N s_N) = \frac{1}{(N!)^{1/2}} \begin{vmatrix} \phi_1(\vec{r}_1 s_1) & \phi_1(\vec{r}_2 s_2) & \cdots & \phi_1(\vec{r}_N s_N) \\ \phi_2(r_1 s_1) & \phi_2(r_2 s_2) & \cdots & \phi_2(r_N s_N) \\ \vdots & \vdots & & \vdots \\ \phi_N(r_1 s_1) & \cdots & \cdots & \phi_N(r_N s_N) \end{vmatrix} \qquad (2.16)$$

where the $\phi_i(\vec{r}_j, s_j)$ are single particle "spin-orbitals". Spin-orbitals are a product of a function of the position $\psi_i^s(\vec{r}_j)$ and a function of the spin variable $\alpha_i(s_j)$. The spin-orbitals must be linear independent and if they are orthonormal the equation simplifies greatly. If the Hamiltonian is independent of spin or diagonal in the basis, the expectation values of the Hamiltonian, using Hartree atomic units, is given by,

$$\langle \Phi | \hat{H} | \Phi \rangle = \sum_{i,s} \int d\vec{r}\, \psi_i^{s*}(\vec{r}) \left[-\frac{1}{2}\nabla^2 + V_{ext}(\vec{r}) \right] \psi_i^s(\vec{r}) + E_{II} + D + X \tag{2.17}$$

where the first term groups together the single-body expectation values, which involve a sum over orbitals. The final two terms, D and X, are the direct and exchange interactions among electrons defined as,

$$\frac{1}{2} \sum_{i,j,s_i,s_j} \int d\vec{r} d\vec{r}'\, \psi_i^{s_i *}(\vec{r}) \psi_j^{s_j *}(\vec{r}') \frac{1}{|\vec{r} - \vec{r}'|} \psi_i^{s_i}(\vec{r}) \psi_j^{s_j}(\vec{r}') \tag{2.18}$$

and

$$-\frac{1}{2} \sum_{i,j,s} \int d\vec{r} d\vec{r}'\, \psi_i^{s*}(\vec{r}) \psi_j^{s*}(\vec{r}') \frac{1}{|\vec{r} - \vec{r}'|} \psi_j^{s}(\vec{r}) \psi_i^{s}(\vec{r}') \tag{2.19}$$

respectively. Here the $i = j$ "self-interaction" is included, but cancels in the sum of direct and exchange terms.

The approach of the Hartree-Fock is to minimize the total energy. The energy can be minimized with the restriction that it has the form of equation 2.13. Now if the spin functions are quantized along an axis, the variation for each spin will yield the Hartree-Fock equations,

$$\varepsilon_i^s \psi_i^s(\vec{r}) = \left[-\frac{1}{2}\nabla^2 + V_{ext}(\vec{r}) + \sum_{j,s_j} \int d\vec{r}' \psi_j^{s_j *}(\vec{r}') \psi_j^{s_j}(\vec{r}') \frac{1}{|\vec{r} - \vec{r}'|} \right] \psi_i^s(\vec{r})$$

$$- \sum_j \int d\vec{r}' \psi_j^{s*}(\vec{r}') \psi_i^s(\vec{r}') \frac{1}{|\vec{r} - \vec{r}'|} \psi_j^s(\vec{r}) \qquad (2.20)$$

where the *exchange term* is summed over all orbitals of the same spin. The exchange term is an integral operator such that it is orthogonal for opposite spins. Thereby when $i = j$ the exchange term cancels with the Coulomb repulsion term. This prevents an electron from interacting with itself which was a correction to the Hartree equations. Numerical methods based on the Hartree-Fock method can be completed in a self-consistent loop. It should be noted that the Hartree-Fock equations can be solved directly only in special cases such as the homogenous electron gas and spherically symmetric atoms [24].

2.3 Density Functional Theory

Density Functional Theory (DFT) is a theory of correlated many-body systems. It is widely used in Quantum Chemistry, Solid-State and Atomic and Molecular Physics. Since its inception it has seen great interest in utilizing and improving the density functional approach. It evolution began in 1927 with Thomas and Fermi, then the theorems of Hohenberg and Kohn made it justifiable, and the Kohn-Sham approach in 1965 made density functional theory practical and widely used today.

The original density functional theory was proposed by L.H Thomas and E. Fermi in 1927. In their approach the kinetic energy of the system of electrons is approximated as a functional of the density. This treated the electrons as non-interacting in a homogeneous

gas with a density equal to the local density at any given point. Later in 1930 Dirac formulated the local approximation for exchange which leads to the energy functional for electrons in an external potential $V_{ext}(\vec{r})$,

$$\mathrm{E}_{TF}[\rho] = C_1 \int d^3 r \rho(\vec{r})^{\frac{5}{3}} + \int d^3 r V_{ext}(\vec{r})\rho(\vec{r}) + C_2 \int d^3 r \rho(\vec{r})^{\frac{4}{3}} + \frac{1}{2}\int d^3 r d^3 r' \frac{\rho(\vec{r})\rho(\vec{r}')}{|\vec{r}-\vec{r}'|} \tag{2.21}$$

where the first term is the local approximation to the kinetic energy, the third term is the local exchange, the last term is the classical Hartree energy and C_1 and C_2 are defined as,

$$C_1 = \frac{3}{10}(3\pi^2)^{\frac{2}{3}} \tag{2.22}$$

and

$$C_2 = -\frac{3}{4}\left(\frac{3}{\pi}\right)^{\frac{1}{3}} \tag{2.23}$$

respectively.[28]

The ground state density can be found by minimizing the functional $E_{TF}[\rho]$ for all possible $\rho(\vec{r})$ with the constraint on the total number of electrons

$$\int d^3 r \rho(\vec{r}) = N\,. \tag{2.24}$$

The solution can be achieved by using the method of Lagrange multipliers where the Lagrange multiplier is the Fermi energy. However this approach contained approximations that are too crude and was lacking the essential physics and chemistry, such as shell structures of atoms and binding of molecules to be used. Therefore it fell short of being useful in describing electrons in matter.

Hohenberg and Kohn took the approach to make the density functional theory as an exact theory of many-body systems. The Hohenberg-Kohn theorems became the basis of density functional theory. In 1964 Hohenberg and Kohn legitimized the use of the electron density as a basic variable with the first of two theorems. Theorem I states that for any system of interacting particles in an external potential $V_{ext}(\vec{r})$, the potential is determined uniquely by the ground state particle density $\rho(\vec{r})$, except for a constant. Since the density determines the number of electrons, then the density also determines the ground state wave function Ψ and inherently all other electronic properties. The second theorem provides the energy variational principle. Theorem II states: a universal functional $F_{HK}[\rho]$ for the energy E[ρ] in terms of the density $\rho(\vec{r})$ can be defined, valid for any external potential $V_{ext}(\vec{r})$. For any particular external potential, the exact ground state energy of the system is the global minimum value of this functional, and the density $\rho(\vec{r})$ that minimizes the functional is the exact ground state density $\rho_0(\vec{r})$. These two theorems proposed by Hohenberg-Kohn were the foundation of a self-consistent method involving independent particles. However, the Kohn-Sham method turned the density functional theory into an useful tool to perform rigorous calculations [28].

The Kohn-Sham approach replaces the interacting many-body system that obeys the Hamiltonian with an auxiliary system that can be easily solved. The Kohn-Sham *ansatz* assumes that the ground state density of the original system is equal to some non-interacting system. What this does is lead to equations for the non-interacting system that are equivalent to the density of the original interacting system. These equations are

solvable with the difficult many-body terms in an exchange-correlation functional of the density. Then by solving these equations the end result is a ground state density and energy of the original interacting system. This results in the accuracy of the answer being controlled by the approximations in the exchange-correlation functional.

In order understand what Kohn and Sham did let's start by first realizing that the actual calculations are performed on the auxiliary system. The auxiliary system is defined by the effective Hamiltonian

$$\hat{H}^s_{KS} = -\frac{1}{2}\nabla^2 + V^s_{KS}(\vec{r}) \tag{2.25}$$

with the potential being

$$V^s_{KS}(\vec{r}) = V^s_{ext}(\vec{r}) + V_{Hartree}(\vec{r}) + V^s_{xc}(\vec{r}). \tag{2.26}$$

For a system of N independent electrons that obey this Hamiltonian, the ground state has one electron in each of the N_s orbitals (ψ_i) with the lowest eigenvalues (ε^i_s) of the Hamiltonian. The density of this system is given by

$$\rho(\vec{r}) = \sum_s \rho(\vec{r}, s) = \sum_{i=1}^{N^s} \sum_s \left|\psi^s_i(\vec{r})\right|^2 \tag{2.27}$$

and the independent-particle kinetic energy T_s,

$$T_s = \frac{1}{2}\sum_s \sum_{i=1}^{N} \left\langle \psi^s_i \middle| \nabla^2 \middle| \psi^s_i \right\rangle . \tag{2.28}$$

Then the classical Coulomb interaction energy of the density interacting with itself is defined as the Hartree energy

$$E_{Hartree}[\rho] = \frac{1}{2}\int d^3r d^3r' \frac{\rho(\vec{r})\rho(\vec{r}')}{|\vec{r} - \vec{r}'|}. \tag{2.29}$$

The Kohn-Sham approach utilizes the Hohenberg-Kohn definition of the universal functional and rewrites the expression for the ground state energy. The resulting expression is written in the form

$$E_{KS} = T_s[\rho] + \int d\vec{r}\, V_{ext}(\vec{r})\rho(\vec{r}) + E_{Hartree}[\rho] + E_{II} + E_{xc}[\rho]. \tag{2.30}$$

Where the $V_{ext}(\boldsymbol{r})$ is the external potential due to the nuclei and any other external fields and E_{II} is the interaction between the nuclei. The independent-particle kinetic energy T_s is given explicitly as a functional of orbitals. The exchange-correlation energy E_{xc} is the final term on the right-hand side of the equation. The exchange-correlation energy takes into account the many-body effects of the exchange and correlation. The expression for the exchange-correlation energy is

$$E_{xc}[\rho] = F_{HK}[\rho] - (T_s[\rho] + E_{Hartree}[\rho]). \tag{2.31}$$

The exchange-correlation functional can be approximated as a local or nearly local functional of the density in the form

$$E_{xc}[\rho] = \int d\vec{r}\,\rho(\vec{r})\varepsilon_{xc}([\rho],\vec{r}) \tag{2.32}$$

where the $\varepsilon_{xc}([\rho],\vec{r})$ is the exchange-correlation density and depends only on the density. The exchange-correlation density can be expressed via

$$\varepsilon_{xc}([\rho],\vec{r}) = \frac{1}{2}\int d^3r' \frac{\overline{\rho}_{xc}(\vec{r},\vec{r}')}{|\vec{r}-\vec{r}'|}. \tag{2.33}$$

The well known Kohn-Sham equations, (2.25) and (2.26) have an independent-particle form with a potential that must be found self-consistently with the resulting density. If the exact functional $E_{xc}[\rho]$ were known, this would lead to the exact ground

state density and energy for the interacting system.[29] This makes one of the most crucial quantities in the Kohn-Sham equations the exchange-correlation energy.[24]

There are relevant approximate exchange-correlation functionals in current use today. They include local density approximations (often referred to the local spin density approximation), generalized-gradient approximations, orbital-dependent functionals, and hybrid functionals. The local density approximation (LDA) is simply an integral over all space with the exchange-correlation density at each point assumed to be the same as in a homogeneous electron gas. The generalized gradient approximation (GGA) is a term used to describe a variety of ways proposed for functions that modify the behavior at large gradients in such a way to preserve desired properties. Various forms of generalized-gradient approximations have been proposed over the years and include Becke (B88), Perdew and Wang (PW91), and Perdew, Burke, and Enzerhof (PBE). Hybrid functionals are a combination of orbital-dependent Hartree-Fock and an explicit density functional such as the three-parameterized B3LYP.[24]

The long time problem with the DFT formalism has been the self-interaction seen in many functionals for exchange and correlation. Within the Hartree-Fock theory, the electron self-interaction is cancelled due to the exact treatments of exchange. However, this is not true for the approximations made to the exchange-correlation functional and since these terms involve large Coulomb interactions the errors can be extensive. In order to correct this unphysical self-interaction several methods add "self-interaction corrections".[24, 28]

Density functional theory is a powerful tool in determining not only the electronic structure, but can be used to determine the optical properties as well. In order to determine the optical properties of clusters one must first understand that in the full many-body problem excitations are described in terms of response functions (χ). Response functions determine the response of the system to external perturbations and excitation energies in the response. Therefore it is important for the theory to have the density response function within the Kohn-Sham framework. Indeed, the Time-dependent density-functional theory (TDDFT) does just that. It is important in the determination of excitation spectra and optical properties [24]. It has been widely used in theoretical determination of optical spectra in both small and large clusters. The formal structure can be derived beginning from the action principle,

$$\frac{\delta A}{\delta \rho(\vec{r},t)} = 0 \tag{2.34}$$

where

$$A = \int_0^{t_1} dt \langle \Psi(t) \left| i\frac{d}{dt} - \hat{\mathrm{H}}(t) \right| \Psi(t) \rangle . \tag{2.35}$$

Now if the idea of replacing the density with the density of independent particles, this will lead to the time-dependent Kohn-Sham density functional theory TDDFT. In the TDDFT there is a time-dependent Schrödinger-like equation

$$i\hbar \frac{d\psi_i(t)}{dt} = \hat{\mathrm{H}}(t)\psi_i(t) \tag{2.36}$$

where the effective Hamiltonian is,

$$\hat{H}_{eff}(t) = -\frac{1}{2}\nabla^2 + V_{ext}(\vec{r},t) + \int \frac{\rho(\vec{r},t)}{|\vec{r}-\vec{r}'|} d\vec{r}' + V_{xc}[\rho](\vec{r},t) \tag{2.37}$$

where $V_{xc}[\rho](\vec{r},t)$ is a function of ***r*** and t, as well as a functional of $\rho(\mathbf{r}', t')$. So far the work to date has used approximations where the exchange-correlation potential is the time-independent functional of the density $V_{xc}[\rho(t)]\mathbf{r}$.[24]

The relation between density and a response function can be expressed by

$$\delta\rho(\vec{r},\omega) = \int d\vec{r}'\chi(\vec{r},\vec{r}';\omega)\delta v(\vec{r}',\omega) \tag{2.38}$$

where the exact density-density response function (χ) has a spectral representation. In the case of the Kohn-Sham approach, the time-dependent density response can be obtained through the self-consistent equation:

$$\delta\rho(\vec{r},\omega) = \int d\vec{r}'\chi(\vec{r},\vec{r}';\omega)\delta v_{eff}(\vec{r}',\omega) \tag{2.39}$$

where

$$\delta v_{eff}(\vec{r},\omega) = \delta v(\vec{r},\omega) + \int d\vec{r}' \frac{\delta\rho(\vec{r}',\omega)}{|\vec{r}-\vec{r}'|} + \delta v_{xc}(\vec{r},\omega) \tag{2.40}$$

These self-consistent equations are reliant on the density being v-representable and noninteracting.[28] A prescription on how to calculate a photabsorption spectrum is as follows: If on has a wave functions of the system in the Kohn-Sham formalism and applies a perturbation of the form $\delta v_{exto}(\mathbf{r},t) = -\kappa_0 r_v \delta(t)$. The amplitude $\kappa 0$ must be small in order to keep the response of the system linear. This perturbation excites all frequencies of the system with equal weight. Then the Kohn-Sham orbitals can be propagated for a finite time and the dynamical polarizability can then be obtained from equation 2.41

$$\alpha_\gamma(\omega) = -\frac{1}{\kappa_0}\int d^3 r r_\gamma \delta\rho(\vec{r},\omega) \qquad (2.41)$$

In equation 2.41 $\delta\rho(\vec{r},\omega)$ stands for the time Fourier transform of $\rho(\vec{r},t)-\tilde{\rho}(\vec{r})$ where the last terms is the ground-state density of the system. This method has been used in successfully to calculate the photabsorption spectrum of several finite systems. [30] For the time-dependent density functional theory, the simplest approximation is the spherical jellium that ignores the atomic structure, but leads to the correct general features of the optical spectra.[24]

The investigation of the SiO clusters are based on first principle calculations using density-functional theory and the generalized gradient approximation for exchange correlation. Various GGA functionals were implemented and compared with previous theoretical and experimental results to determine the best functional to use for exchange correlation. The energies, geometries of various Si_nO_n, Si_nO_{n+1}, Si_nO_{n-1} ($1 \leq n \geq 12$) clusters were calculated using a linear combination of atomic orbitals-molecular orbital approach. The atomic orbitals were represented by the double-zeta valence polarization basis set [31]. The calculations were carried out using the deMon code developed by Köster and co-workers [32]. An auxiliary basis set was used for the variational fitting of the Coulomb potential [33] and numerical integration of the exchange-correlation energy and potential were performed on an adaptive grid [34]. Many initial configurations for the optimization of structures were used in order to prevent getting trapped in a local minimum of the potential energy surface. The structures were fully optimized without constraints [35]. The optical properties were examined using the Gaussian 03 code [36]. The B3LYP exchange

correlation functional was used because it is known to provide better optical absorption energies. A 6-31+G* basis set using the same generalized gradient as described above was used for structure optimization.

CHAPTER 3 Results on Silicon Oxide Clusters

3.1 Si_nO_n (n = 1-12) Clusters

Figure 3.1 shows the structures for neutral Si_nO_n (n = 1-5). The ground states for structures 2-4 are open ring structures. The Si-O bond length of these structures is 1.73 Å and is longer than the SiO bond length of 1.55 Å. The Si_5O_5 structure marks the beginning of a silicon core. The core consists of two or more Si-Si bonds in any given structure. The Si_5O_5 structure has one five-membered ring and one six-membered ring that share one silicon atom. The lone Si-Si bond is 2.47 Å in length, while the Si-O bonds range from 1.69 to 1.71 Å in length. As the cluster size begins to grow, so too does the silicon core. Si_6O_6 has a core of three silicon atoms, while Si_8O_8 has a distinct planar core of four silicon atoms (Figure 3.2). The silicon cores are surrounded by a sheath of SiO_2 molecules. This trend continues up to $Si_{12}O_{12}$ where the interior core becomes cage-like in structure. The cage is then surrounded by the SiO_2 molecule on various sides (Figure 3.3).

Many of these structures are unique in the fact that not only do these structures contain Si-Si cores and SiO_2 sheaths, but there is a predominance of five and six-membered rings throughout the entire series. The presence of the five and six-membered rings can be seen beginning at Si_5O_5 and continue throughout. The five membered rings have an oxygen-deficient to silicon ratio, while the six-membered ratio is 1. In each of

these cases, the bond lengths range from 1.68 to 1.71 Å and 2.27 to 2.39 Å for Si-O and Si-Si respectively.

The stability of pure Si_nO_n clusters is important in gaining an understanding into the geometries and any highly stable species. Therefore the atomization energy for each cluster was determined. The atomization energy (AE) is defined as the amount of energy it takes to break a cluster into *n*Si and *n*O atoms:

$$AE = nE(Si) + nE(O) - E(Si_nO_n) \qquad (3.1)$$

The atomization energies can be seen in Table 3.1. The atomization energy of SiO is 8.21 eV while SiO_2 has the atomization energy of 12.78 eV or 6.39 eV per SiO bond. However, the Si_2 molecule has a binding energy of 2.45 eV and as such it would be energetically unfavorable for the formation of the Si-Si cores. However, the silicon atom is marked by tetrahedral bonding in bulk while the oxygen atom is divalent. It can be seen that the oxygen atoms are typically bonded to two silicon atoms. As the cluster size increases the interior requires for a greater coordination number, thus silicon fills this requirement. This coordination chemistry is creating the silicon cores and oxygen exterior.

SiO Units	AE	Si-Si bonds	Si-O bonds
2	18.44	2.51	1.74
3	28.93	n/a	1.71
4	38.72	n/a	1.70
5	49.15	2.47	1.69-1.71
6	59.40	2.29-2.49	1.70-1.73
7	70.98	2.43	1.68-1.72; 1.87
8	80.85	2.36	1.70-1.72
9	91.61	2.27	1.76
10	102.70	2.47	1.69-1.71
11	112.99	2.27-2.38	1.68
12	123.64	2.36-2.39	1.72

Table 3.1: Atomization energies (eV) and Silicon bond lengths in angstroms (Å) and Silicon-Oxygen bond lengths also in angstroms for $(SiO)_n$ clusters.

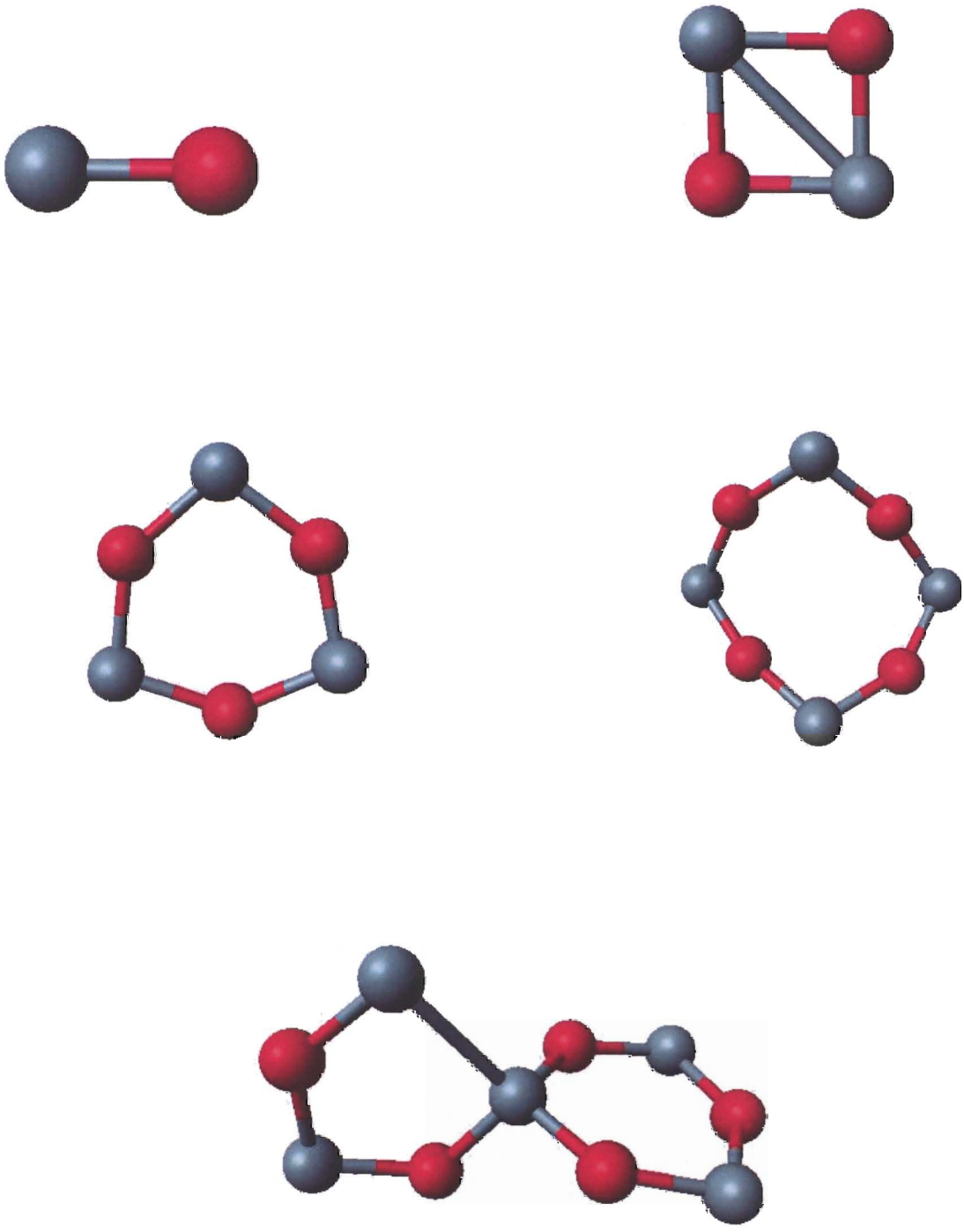

Figure 3.1: Si_nO_n Structures for n = 1-5. Oxygen atoms are red, while silicon atoms are gray in color.

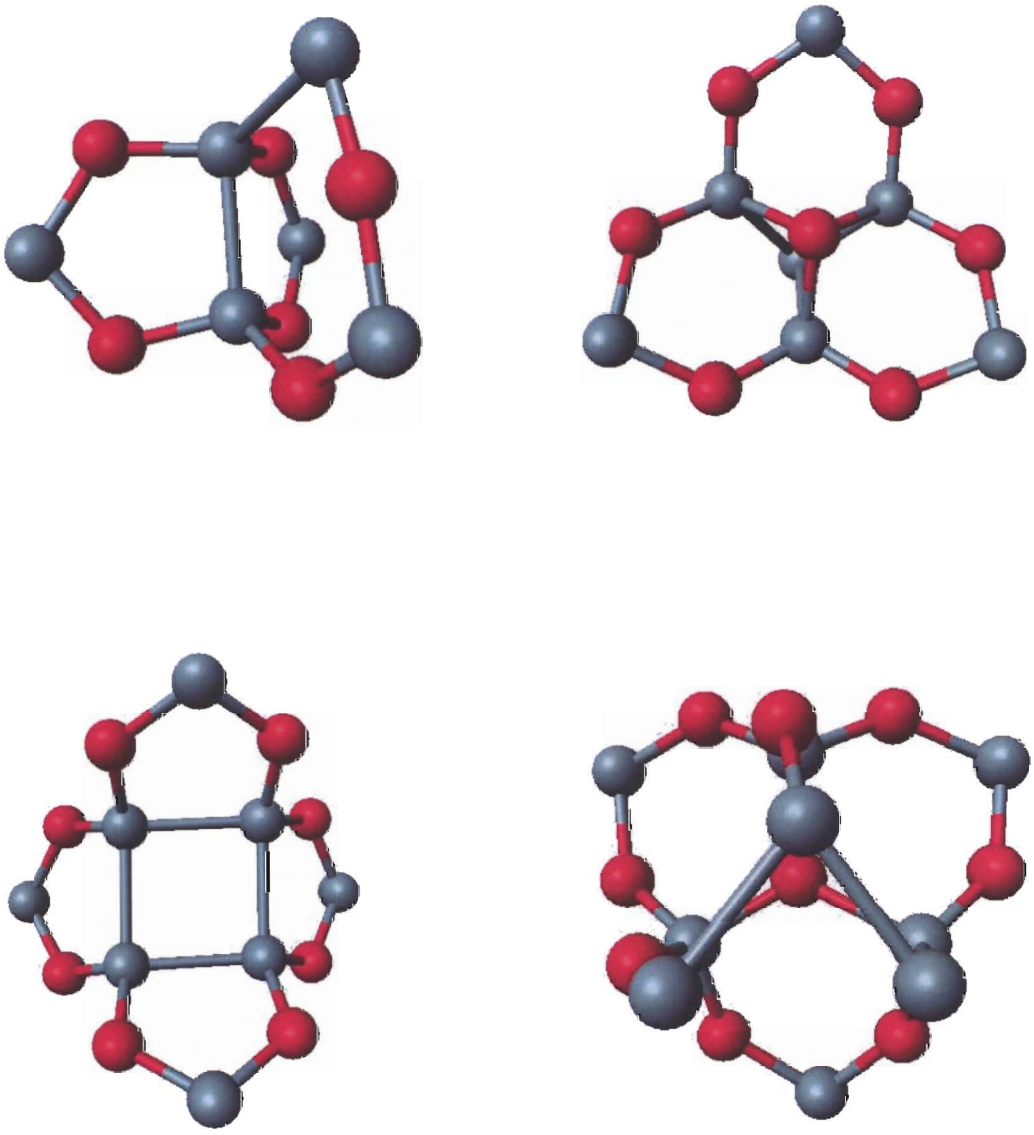

Figure 3.2: Si_nO_n Structures for n = 6-9. Oxygen atoms are red, while silicon atoms are gray in color.

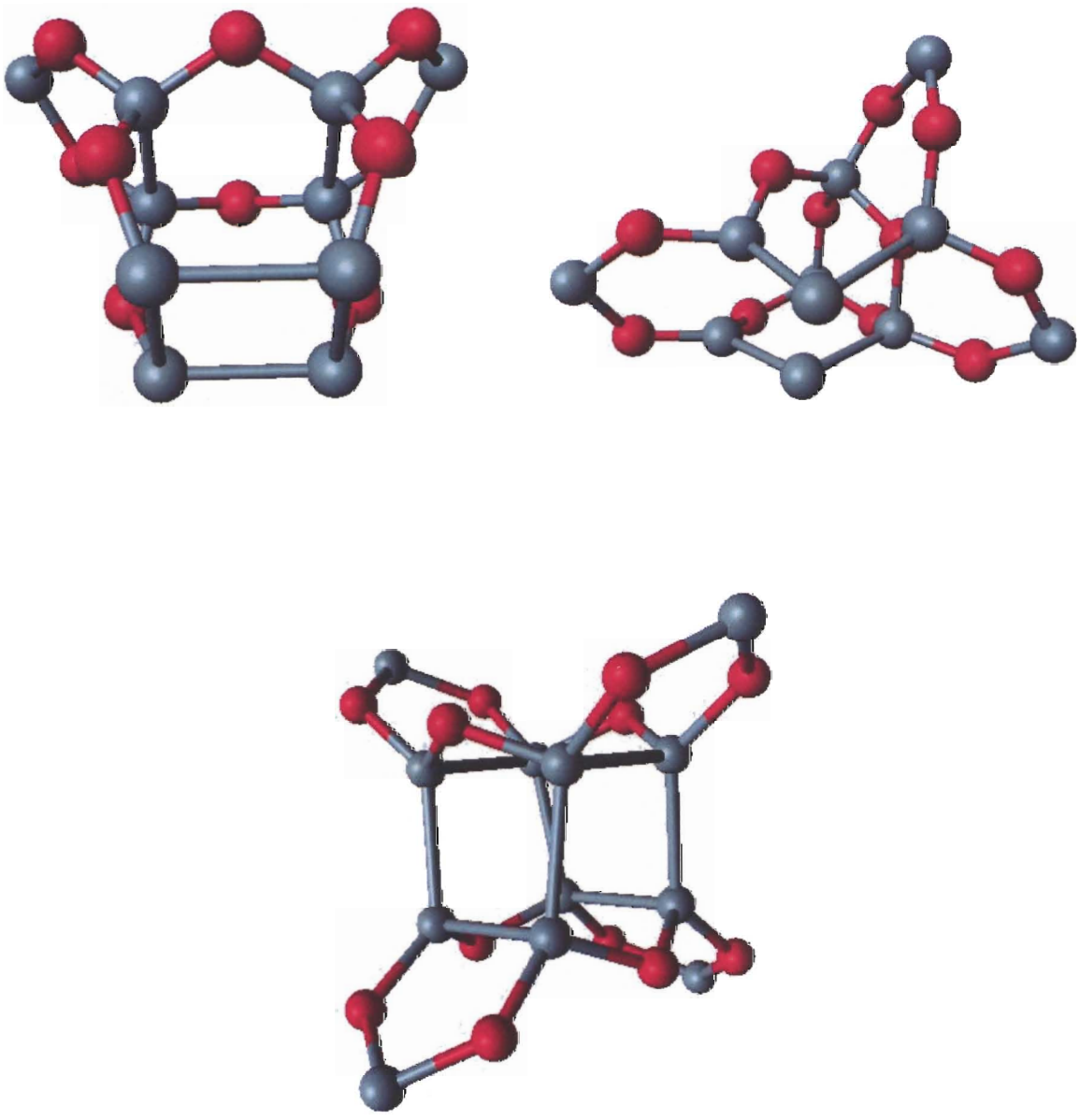

Figure 3.3: Si_nO_n Structures for n = 10-12. Oxygen atoms are red, while silicon atoms are gray in color.

3.2 Energetics & Mechanisms

In order to identify any particular stable species it is important to evaluate the energetics. The stability of pure Si_nO_n clusters were evaluated by looking at the atomization energy (AE), the energy gain (ΔE), defined as the amount of energy gained when adding one SiO unit,

$$\Delta E = E(Si_{n-1}O_{n-1}) + E(SiO) - E(Si_nO_n) \qquad (3.2)$$

as well as the ionization potentials and electron affinities. The energy gain, ionization potentials, and electron affinities can be seen in Table 3.2. The atomization energy increases with size. This is indicative of stability toward atomic constituents. The energy gain plot seen in Figure 3.4 for the pure Si_nO_n clusters show three distinct peaks. These distinct peaks occur where n = 3, 7, and 10, indicating Si_3O_3, Si_7O_7 and $Si_{10}O_{10}$ are highly stable. The largest of these three peaks is Si_7O_7 and this cluster may be considered unusually stable.

Notice in Figure 3.4 there is a large increase from n = 6 to n = 7. This means that Si_6O_6 could be a highly unstable species. If Si_6O_6 is an unstable the question is raised could this lead to fragmentation into silicon rich and oxygen rich clusters? In order to answer this question the ground-state geometries of Si_nO_{n+1} and Si_nO_{n-1} were determined. The issue is to determine any clusters where the energy gained in combining two units is sufficient to break the cluster into an oxygen-rich and a silicon-rich fragment. The energetics of the reaction

$$Si_nO_n + Si_mO_m \rightarrow Si_{n+m-j}O_{n+m-k} + Si_jO_k \qquad (3.3)$$

SiO Units	ΔE	AEA	VIP
2	2.02	0.92	9.04
3	2.28	0.93	8.57
4	1.58	1.46	8.27
5	2.21	1.99	7.69
6	2.05	2.28	7.45
7	3.37	1.87	7.36
8	1.66	2.36	6.68
9	2.25	2.18	6.58
10	3.18	0.69	8.09
11	2.09	2.13	5.19
12	2.51	2.03	7.24

Table 3.2: Energy Gain (ΔE), adiabatic electron affinity (AEA), and vertical ionization potential (VIP) for $(SiO)_n$ clusters n = 2-12.

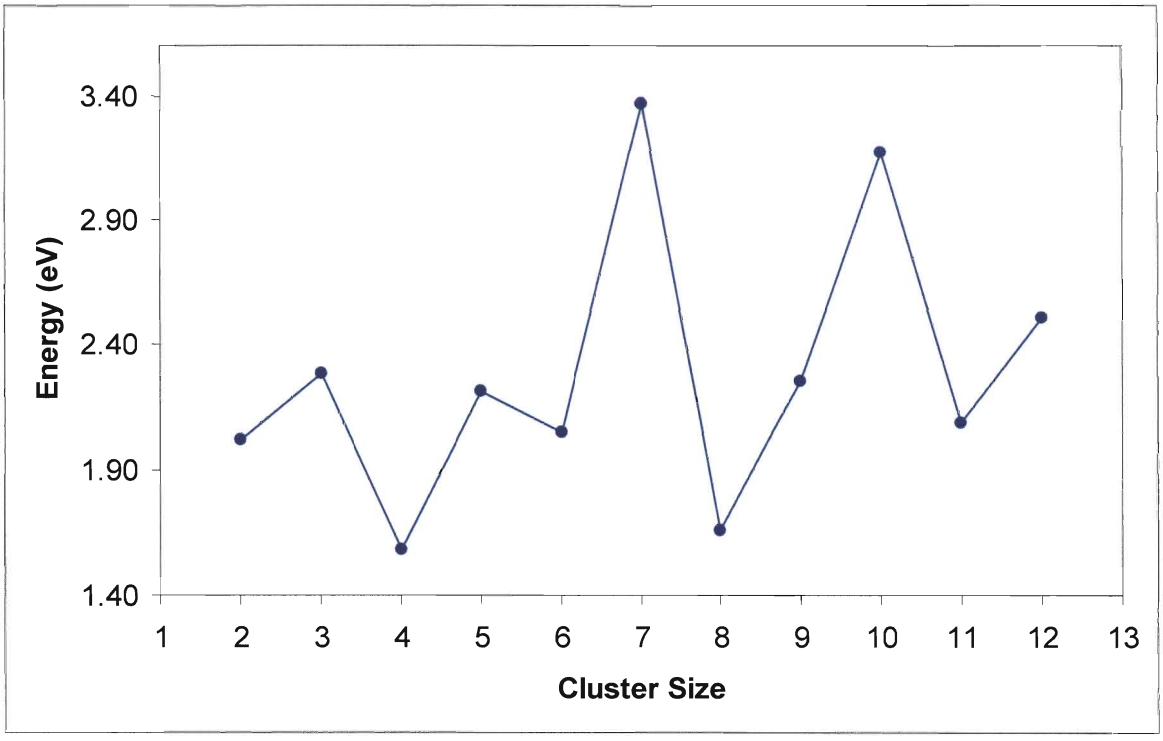

Figure 3.4: Energy Gain (eV) of $(SiO)_n$ clusters where n = 2-12.

were determined using the total binding energy of the ground-state energies. The smallest size where the reaction is energetically favorable is Si_5O_5,

$$Si_5O_5 + Si_2O_2 \rightarrow Si_5O_6 + Si_2O \quad (3.4)$$

$$\Delta E = -0.05 \text{ eV}$$

This leads to the formation of Si_5O_6. It is also shown that Si_6O_6 can generate other oxygen-rich clusters through the following processes,

$$Si_6O_6 + SiO \rightarrow Si_5O_6 + Si_2O \quad (3.5)$$

$$\Delta E = -0.03 \text{ eV}$$

$$Si_6O_6 + Si_2O_2 \rightarrow Si_6O_7 + Si_2O \quad (3.6)$$

$$\Delta E = -0.09 \text{ eV}$$

The formation of Si_5O_6 begins the process for the production of SiO_2. Two processes

$$Si_5O_6 + Si_6O_6 \rightarrow Si_3O_3 + Si_8O_8 \quad (3.7)$$

$$\Delta E = -0.04 \text{ eV}$$

and

$$Si_5O_6 + Si_5O_5 \rightarrow Si_3O_4 + Si_7O_7 \quad (3.8)$$

$$\Delta E = -0.67 \text{ eV}$$

both convert Si_5O_6 to Si_3O_4. This is followed by the processes

$$Si_3O_4 + Si_6O_6 \rightarrow Si_2O_3 + Si_7O_7 \quad (3.9)$$

$$\Delta E = -0.04 \text{ eV}$$

and

$$Si_2O_3 + Si_6O_6 \rightarrow SiO_2 + Si_7O_7 \quad (3.10)$$

$$\Delta E = -0.23 \text{ eV}$$

which are energetically favorable. These processes lead to the formation of SiO_2. There are similar reaction pathways that may be written for Si_6O_7 that is generated in equation 3.6. It is also important to note that the above pathway to SiO_2 is not unique. Many of the larger clusters also lead to SiO_2 through other multi-step processes. The two clusters Si_5O_5 and Si_6O_6 are special because they are the smallest of the clusters that begin and carry out the process of oxygen enrichment. It should be noted that the theoretical calculations are carried out at a temperature of 0 K while the temperatures in the interstellar medium (ISM) range from 4 K to 1300 K. Also the mass outflows from evolved stars is a highly non-equilibrium process and the vibrational temperatures are much less than the kinetic temperatures.

3.3 Optical Properties

The process that produces the extended red emissions is believed to be a photoluminescent one. These emissions have peaks that range from 610 to 820 nm. The blue luminescence that can be seen in the interstellar medium consists of a range from 357 to 486 nm. The electronic structure calculations can give insight into whether or not these silicon oxide clusters may lead to these types of emissions. Figure 3.5 shows the Highest occupied molecular orbital - Lowest unoccupied molecular orbital (HOMO-LUMO) gap range for Si_nO_n clusters as well as Si_nO_{n+1} and Si_nO_{n-1} clusters. The gap ranges from 0.84 to 3.84 eV. Since this falls within the emission range, it may be possible for these clusters to contribute to the emissions seen in various environments.

In order to further examine the optical properties of these clusters, time-dependent density functional (TD-DFT) calculations were performed using procedure described in section 2.3. The final results for the optical gaps for the silicon systems of Si_nO_n, Si_nO_{n+1}, and Si_nO_{n-1} can be seen in Figure 3.6. The optical gaps range from 225 to 850 nm for Si_nO_n and Si_nO_{n+1}. If the Si_nO_{n-1} clusters are included, the range extends to 1150 nm. Clearly this range is within the extended red emission and blue luminescence range. However, this is not an emission spectra, but represents an absorption spectra. In order to examine the emission spectra relaxations of the clusters must be further examined.

A very powerful tool into the composition of the interstellar medium is the infrared (IR) spectra. Therefore the infrared spectra for the Si_nO_n clusters were determined. The IR spectra for the series of Si_nO_n (n = 1-12) clusters yield intense peaks from 600 to 700 cm^{-1}. These seem to be in agreement with the expected infrared spectra shown in the article Li and Draine [36]. These vibrational modes show further illustrate the possibility for these clusters to be a contributor to the extended red emissions seen in the interstellar medium.

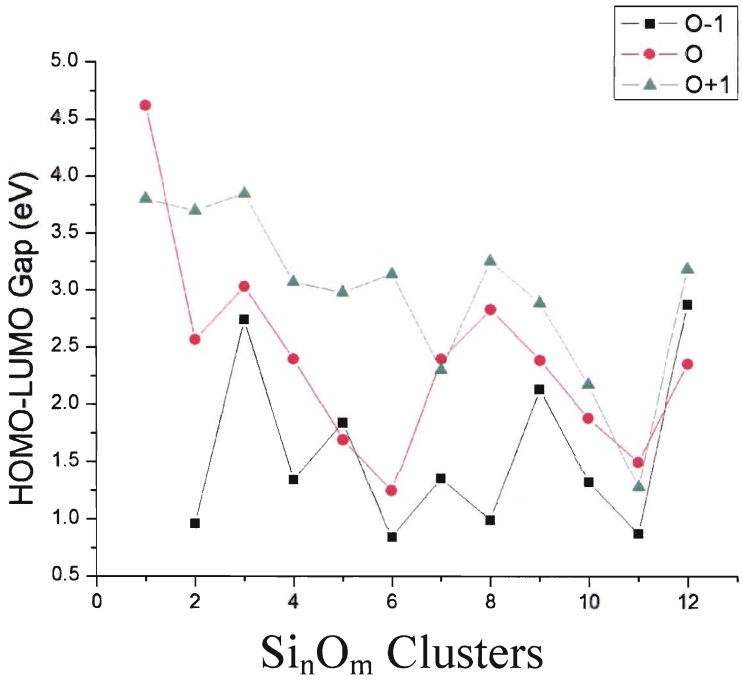

Figure 3.5: HOMO-LUMO gaps for Si_nO_m Structures.

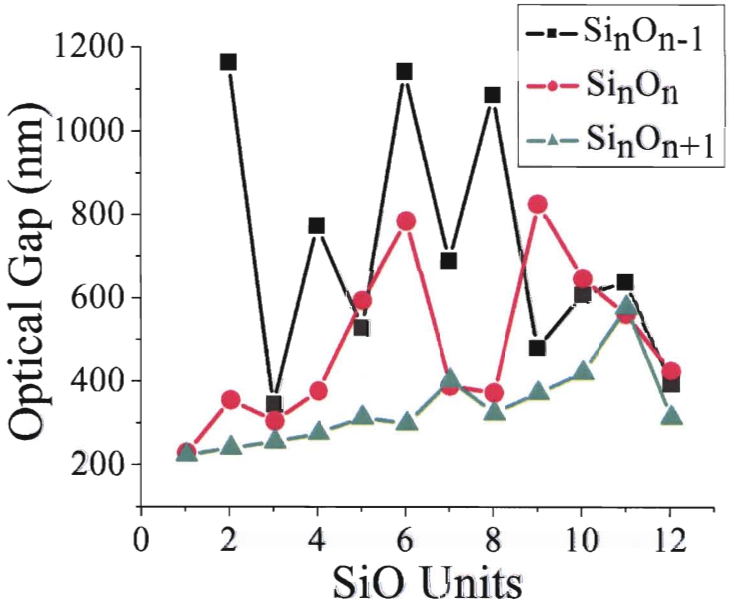

Figure 3.6: Optical gaps for Si_nO_m Clusters.

CHAPTER 4 Conclusions

4.1 Summary

In summary, it is shown there is an energetically mechanism for the formation of oxygen rich species with SiO_2 as a final cluster through the collisions of SiO molecules. The $(SiO)_x$ clusters begin as ring structures and proceed to form silicon-silicon cores. The growth of these structures eventually leads to the formation of silicon cages surrounded by five-membered rings. The cores from the silicon oxide clusters may be one originating source of the extended red emissions seen in the diffuse galactic background. Also it has been shown that Si_3O_3, Si_7O_7 and $Si_{10}O_{10}$ are magic clusters in the series of silicon monoxide clusters.

Even though this work has provided answers for several questions, there are many unanswered questions still to be investigated. (1) Is SiO_2 growth facilitated by agglomeration? (2) Does the prominence of rings and cages seen in the Si_nO_n clusters continue for sizes where $n > 12$? (3) Do these structures hold true at larger temperatures? (4) Is there a mechanism for the formation of larger silicon to oxygen ratios from silicon oxide clusters? (5) What does the emission spectra for these clusters truly look like? As one can see this work is only the beginning to understanding not only the mechanisms and formation of cluster-assembled materials, but may eventually lead to better understanding formation processes of our galaxy.

Literature Cited

Literature Cited

[1] JA Cortes, M Wilson, E Condliffe *et al.* *Journal of Petrology* **47**, 7 (2006).

[2] EF Van Dishoeck, *Annual Review of Astronomy and Astrophysics* **42**, 119 (2004).

[3] J.A. Nuth and B. Donn. *J. Chem Phys* **78**, 1618 (1983).

[4] B. Donn and J.A. Nuth. *J. Astrophys* **288**, 187 (1985).

[5] H.P. Gail and E. Sedlmayr. *Astron. Astrophys* **166**, 225 (1986).

[6] AN Witt and TL Smith. *Astrophys Journal* **565**, 304 (2002).

[7] J. Bradley, ZR Dai, R Erni, N Browning, *et al.* *Science* **307**, 244-247 (2005).

[8] CM Lisse, J VanCleve, AC Adams, MF A'Hearn, *et al.* *Science* **313**, 635-640 (2006).

[9] JR Brucato, L Colangeli, V Mennela, P Palumbo, and E Bussoletti. *Planetary and Space Science* **47**, 773-779 (1999).

[10] GD Schmidt, M Cohen, and B Margon. *Astrophysical Journ.* **239**, L133 (1980).

[11] BT Draine *Annual Review Astronomy and Astrophysics.* **41**, 241 (2003).

[12] AN Witt, KD Gordon, UP Vijh, PH Sell, TL Smith and R Xie. *Astrophysical Journal* **636**, 303 (2006).

[13] UP Vijh, AN Witt, and KD Gordon. *Astrophysical Journal* **606**, L65 (2004).

[14] AN Witt, KD Gordon, and D Furton. *Astrophysical Journal* **501**, L111-L115 (1998).

[15] M. Cardona and P. Yu *Fundamentals of Semiconductors* 3^{rd} *ed.* Springer, 2001).

[16] Z. Zhou *et al.* *Nanoletters* **3**, 2 (2003).

[17] N. Wang, YH Tang, YF Zhang, *et al. Phys Rev. B* **58**, 24 (1998).

[18] G Jia, M Kittler, Z Su, D Yang, and J Sha. *Phys. Stat. Sol.* **203**, 8 (2006).

[19] SK Nayak, BK Rao, SN Khanna, and P Jena. *J. Chem Phys* **109**, 4 (1998).

[20] QJ Zhang, ZM Su, WC Lu, CZ Wang, and KM Ho. *J. Chem Phys A* **110**, 8151-8157 (2006).

[21] RQ Zhang, MW Zhao, and ST Lee. *Phys Rev. Lett.* **93**, 9 (2004).

[22] GH Kim, JH Kim, KA Jeon, and SY Lee. *J. Vac. Sci. Technol A* **23**, 4 (2005).

[23] DA Dixon and JL Gole, *J. Phys. Chem. B* **109**, 14830-14835 (2005).

[24] Richard M. Martin *Electronic Structure: Basic Theory and Practical Methods.* Cambridge University Press 2004.

[25] David Chandler *Introduction to Modern Statistical Mechanics.* Oxford 1987);

[26] TL Hill *An Introduction to Statistical Thermodynamics.* Dover 1986).

[27] NW Ashcroft and ND Mermin *Solid State Physics.* Saunders College Publishing, 1976.

[28] Robert G. Parr and Weitao Yang *Density-Functional Theory of Atoms and Molecules.* Oxford University Press 1989).

[29] W. Kohn and L.J. Sham, *Phys. Rev.* **140**, A1133 (1965).

[30] Marques, M.A.L. and Gross E.K.U., *Annu. Rev. Phys. Chem.* **55**, 427-455 (2004).

[31] N Godbout, DR Salahub, J Andzelm, E Wimmer, *Can. J. Chem.* **70**, 560 (1992).

[32] Köster, A. M.; Calamininci, P.; Flores, R.; Geudtner, G.; Goursot, A.; heine, T.; Janetzko, F.; Patchkovskii, S.; Reveles, J. U.; Vela, A.; Salahub, Dr. deMon, NRC, Canada, 2004. Avaiable from: http://www.deMon-software.com.

[33] AM Köster, JU Reveles, and JM del Campo. *J. Chem. Phys.* **121**, 3417 (2004).

[34] AM Köster, R Flores-Moreno, and JU Reveles. *J. Chem. Phys.* **121**, 681 (2004).

[35] Reveles, J. U.; Köster, A.M. *J. Comput. Chem.* **25**, 1109 (2004).

[36] Frisch, M. J.; Trucks, G. W.; Schlegel, H. B.; Scuseria, G. E.; Robb, M. A.; Cheeseman, J. R.; Montgomery, J. A., Jr.; Vreven, T.; Kudin, K. N.; Burant, J. C.; Millam, J. M.; Iyengar, S. S.; Tomasi, J.; Barone, V.; Mennucci, B.; Cossi, M.; Scalmani, G.; Rega, N.; Petersson, G.A.; Nakatsuji, H.; Hada, M.; Ehara, M.; Toyota, K.; Fukuda, R.; Hasegawa, J.; Ishida, M.; Nakajima, T.; Honda, Y.; Kitao, O.; Nakai, H.; Klene, M.; Li, X.; Knox, J. E.; Hratchian, H. P.; Cross, J. B.; Bakken, V.; Adamo, C.; Jaramillo, J.; Gomperts, R.; Stratmann, R.E.; Yazyev, O.; Austin, A. J.; Cammi, R.; Pomelli, C.; Ochterski, J.W.; Ayala, P. Y.; Morokuma, K.; Voth, G. A.; Salvador, P.; Dannenberg, J. J.; Zakrzewski, V. G.; Dapprich, S.; Daniels, A. D.; Strain, M. C.; Farkas, O.; Malick, D. K.; Rabuck, A. D.; Raghavachari,K.; Foresman, J. B.; Ortiz, J. V.; Cui, Q.; Baboul, A. G.; Clifford, S.; Cioslowski, J.; Stefanov, B. B.; Liu, G.; Liashenko, A.; Piskorz, P.; Komaromi, I.; Martin, R. L.; Fox, D. J.; Keith, T.; Al-Laham, M. A.; Peng, C. Y.; Nanayakkara, A.; Challacombe, M.; Gill, P. M. W.; Johnson, B.; Chen, W.; Wong, M. W.; Gonzalez, C.; Pople,J. A. *Gaussian 03*; Gaussian, Inc.: Wallingford, CT, 2004.

[37] A Li and BT Draine. *The Astrophys Journ.* **564**, 803-812 (2002).

VITA

Peneé Armaize Clayborne was born January 26, 1978 in Rocky Mount, Virginia. After graduating from Franklin County High School, she attended Radford University in Radford, Virginia, where she earned a B.S in Physical Science with a concentration in Physics. During her undergraduate years, she was involved in astronomy research at Radford University's observatory and participated in the Material Science REU program at James Madison University. Her work at James Madison University allowed her to present a poster at the 223rd National Meeting of the American Chemical Society in Orlando, FL in March of 2002, entitled "Temperature-programmed desorption: FTIR investigation of primary alcohols adsorbed on bohomite", which was later published in *Applied Catalysis A* in 2004. Upon graduation from Radford University, Peneé worked for two years at Federal Express Ground Division as a Service Manager, before pursuing a Master of Science degree at VCU.

While pursuing her M.S., Miss Clayborne was privileged to work with Dr. S.N Khanna's Atomic Physics Theory Group. While working in Dr. Khanna's group she had various achievements and opportunities. Her work on silicon oxide resulted in a publication entitled "Silicon Oxide Nanoparticles Reveal the Origin of Silicate Grains in Circumstellar Environments" in *Nano Letters* in 2006. She gave a presentation at the APS March meeting in 2006 entitled "Single and Multiple Rings, and Cages in $(SiO)_x$ Clusters". Peneé was invited to present this research at Radford University (February 2006) and James Madison University (August 2006). In December 2006, she successfully completed her Master of Science in Physics at Virginia Commonwealth University in Richmond, Virginia. Peneé is looking forward to continuing her research while pursuing her dream of obtaining a Ph.D and mentoring other African-American students in the sciences.